BBA - Molecular Basis of Disease 1865 (2019) 107–114

Contents lists available at ScienceDirect

BBA - Molecular Basis of Disease

journal homepage: www.elsevier.com/locate/bbadis

A *FBN1* 3′UTR mutation variant is associated with endoplasmic reticulum stress in aortic aneurysm in Marfan syndrome

Anna-Maria Siegert[a,1], Gerardo García Díaz-Barriga[a,b,c,d,1], Anna Esteve-Codina[e,f], Miquel Navas-Madroñal[g,h], Darya Gorbenko del Blanco[a,b], Jordi Alberch[a,b,c,d], Simon Heath[e,f], María Galán[g,h,2], Gustavo Egea[a,b,i,*,2]

[a] Department of Biomedical Sciences, School of Medicine and Health Sciences, University of Barcelona, Barcelona 08036, Spain
[b] Institute of Biomedical Investigation August Pi i Sunyer (IDIBAPS), 08036 Barcelona, Spain
[c] Institute of Neurosciences, UBNeuro, University of Barcelona, 08036 Barcelona, Spain
[d] Centers for Networked Biomedical Research (CIBERNED), Instituto Carlos III, 28031 Madrid, Spain
[e] CNAG-CRG, Centre for Genomic Regulation (CRG), Barcelona Institute of Science and Technology (BIST), 08028 Barcelona, Spain
[f] Pompeu Fabra University, 08002 Barcelona, Spain
[g] Sant Pau Biomedical Research Institute (IIB-Sant Pau), 08025 Barcelona, Spain
[h] CIBER of Cardiovascular Disease (CIBERCV), ISCIII, 28029 Madrid, Spain
[i] Institute of Nanoscience and Nanotechnology IN2UB, University of Barcelona, 08036 Barcelona, Spain

ARTICLE INFO

Keywords:
Marfan syndrome
ER stress
Fibrillin-1
3′UTR mutations
Aortic aneurysm

ABSTRACT

Marfan syndrome (MFS) is caused by mutations in the protein fibrillin-1 (FBN1) which affects the integrity of connective tissue elastic fibres. The most severe clinical outcome is the formation of ascending aortic aneurysms. *FBN1* mutations are extremely variable and the prediction of disease phenotype and aortic risk is challenging under the prevailing mutation type classification. Finding a better correlation between mutation type and disease development is crucial for patient treatment. By mRNA sequencing of cultured vascular smooth muscle cells derived from control subjects and from the dilated and non-dilated aortic tunica media of MFS patients, we found a scarcely described *FBN1* 3′UTR mutation. This mutation was accompanied by a clear gene ontological endoplasmic reticulum (ER) stress response in the non-dilated aortic zone, which was confirmed by the increased transcriptional expression of *MANF*, *HSPA5*, *SEL1L*, *DDIT3/CHOP* and *CRELD2* as well as protein expression levels of BiP/GRP78, CHOP and sXBP1. Moreover, the ER stress response was accompanied by a decrease in the phosphorylation levels of the protein translation regulator elF2α. In conclusion, we here identify a 3′UTR mutation of *FBN1* in MFS patients, whose molecular mechanism suggest the involvement of the ER stress response in the formation of the aortic aneurysm. Our results emphasise the importance of mutations in non-coding regions and their resulting molecular mechanisms in the development of connective tissue diseases with impact on the cardiovascular system.

1. Introduction

Marfan Syndrome (MFS) is an autosomal dominant disease that affects between 1.5 and 17.2 in 100,000 live births and is associated with mutations in the protein fibrillin-1 (FBN1) [1]. FBN1 is a crucial component of connective tissue elastic fibres and an important extracellular regulator of Transforming Growth Factor-β (TGF-β) activity [2]. The most severe clinical manifestations of MFS arise from cardiovascular system abnormalities characterised by progressive aortic root enlargement and ascending aortic aneurysm [3].

Mutations in *FBN1* are found throughout the entire gene with only 12% of all variants being recurrent. The actual number of mutations might be significantly higher due to the clinically challenging nature of diagnosing MFS or failure to report variants [4]. Mutations in *FBN1* are classified by haploinsufficient (HI) or dominant-negative (DN) protein defects, and correlational studies have attempted to link disease

* Corresponding author at: Department of Biomedical Sciences, School of Medicine and Health Sciences, University of Barcelona, c/ Casanova, 143, 08036 Barcelona, Spain.
E-mail address: gegea@ub.edu (G. Egea).
[1] These authors contributed equally to this work.
[2] Co-senior authors.

https://doi.org/10.1016/j.bbadis.2018.10.029
Received 13 April 2018; Received in revised form 2 October 2018; Accepted 26 October 2018
Available online 30 October 2018
0925-4439/

severity with either mutation type [5]. Despite this categorization, studies are still too underpowered to conclusively evaluate the differential risk of aortic dissection or the need for clinical intervention between groups [6]. For instance, in a recent large-scale study, 37% of MFS patients could not be grouped by their mutation into either HI or DN phenotype which indicates that the prevailing paradigm is lacking a complete phenotype-associated gene profile [7]. Evidently, the large variability of variant mutations is not easily interpreted and variant databases contain confounding information [8]. Furthermore, a significant portion of genetically unresolved cases demonstrates that conventional exon analysis is insufficient to detect and phenotypically associate all disease causing variants [9].

Here we report a non-exonic *FBN1* 3′UTR mutation in vascular smooth muscle cells (VSMC) from MFS patients with aortic phenotype. We show distinct protein and pathway enrichment of the differentially expressed genes (DEGs) indicative of an endoplasmic reticulum (ER) stress response that potentially contributes to aortic aneurysm formation. Thus, our results indicate that non-exonic 3′UTR *FBN1* mutations are potentially relevant in the prediction of MFS disease outcome.

2. Material and methods

2.1. Human tissue collection, ethics statements and subjects

Control ascending aortic tissue was collected from four male heart donors through the organ donation organization at the Hospital Clínic i Provincial (Barcelona, Spain) and Hospital de Bellvitge, L'Hospitalet de Llobregat (Barcelona, Spain). Ascending aortic aneurysm samples were collected from five male MFS patients undergoing aortic aneurysm repair surgery. All patients fulfilled MFS diagnostic criteria according to Ghent Nosology. From each patient we obtained a sample from the dilated zone (d) (corresponding to the sinuses of Valsalva) and the non-dilated (nd) aorta (corresponding to the adjacent distal ascending aorta). The aortae were maintained in cold saline solution or cardioprotective solution before delivery to the laboratory. Human tissues were collected with the required approval from the Institutional Clinical Review Board of Spanish clinical centers, and the patients' written consent conformed to the ethical guidelines of the 1975 Declaration of Helsinki. All aortic tissues described in the manuscript were obtained from Spanish Marfan patients and heart donors. Due to the Spanish Data Protection Act, we did not have access to their clinical history or personal data.

2.2. Vascular smooth muscle cells culture

VSMC from control donors and MFS patients were cultured as stated previously [10]. Briefly, aortic tissue was cut into small pieces and left to adhere to cell culture plates in human VSMC medium. VSMC start to migrate from the tissue within 1–2 weeks and are routinely subcultured until P5.

2.3. mRNA extraction and sequencing of VSMC

RNA was extracted using RNeasy® MiniKit (Quiagen, Hilden, Germany). Total RNA was assayed using Qubit® RNA HS-Assay (Life Technologies) and RNA 6000 Nano-Assay on a Bioanalyzer 2100. The RNASeq libraries were prepared from total RNA using the TruSeq®Stranded mRNA LT Sample Prep Kit. Libraries were sequenced on HiSeq2000 (Illumina, Inc) in paired-end mode with a read length of 2 × 76 bp using TruSeq SBS Kit v4.

2.4. Quantitative RT-PCR

Total RNA was isolated using the TriPure Isolation Reagent (Roche Diagnostics, Indianapolis, IN). Total RNA (1 μg) was reverse transcribed using the High Capacity cDNA Archive Kit (Applied Biosystems, Foster City, CA) with random hexamers. Quantification of mRNA levels was performed by real-time PCR using an ABI PRISM 7900HT sequence detection system (Applied Biosystems, Foster City, CA) and specific primers and probes provided by Applied Biosystems (Assay-on-Demand system) as follows: Mesencephalic Astrocyte Derived Neurotrophic Factor (Manf; Hs00180640_m1), Cysteine-rich with EGF-like domains 2 (Creld2; Hs00360923_g1), Protein sel-1 homolog 1 (Sel1L; Hs01071406_m1), Heat shock 70 kDa protein 5 or 78 kDa glucose-regulated protein (GRP-78) (Hspa5; Hs00607129_gH), Activating transcription factor 4 (Atf4; Hs00909569_g1), Activating transcription factor 6 (Atf6; Hs00232586_m1), Inositol-requiring enzyme 1 (Ern1; Hs00176385_m1), and DNA Damage Inducible Transcript 3 or C/EBP homologous protein (CHOP) (Ddit3; Hs99999172_m1). As endogenous controls glyceraldehyde 3-phosphate dehydrogenase (GAPDH; Hs02786624_g1) and β-Actin (Actb; Hs99999903_m1) were used. Similar results were obtained after normalization to both housekeeping genes.

2.5. Western Blot

Total protein analysis by Western Blot was performed as described previously [10]. Briefly, confluent VSMC were lysed, and 20 μg of total protein were loaded onto SDS-PAGE gels. Protein was transferred to a nitrocellulose membrane, and incubated with antibodies specific to BiP/GRP78, HSP90, (p)eIF2α and eIF2α were purchased from Cell Signalling (Leiden, NL), and antibodies to ATF6 (total and active forms), CHOP and sXBP1 from Novus Biologicals (Bio-Techne LD- RyD systems Europe Ltd., Abingdon, UK). Protein bands were visualized on film using ECL reagent (Santa Cruz, CA, USA) and analysed using Image J software (NIH, MD USA).

2.6. Bioinformatic analysis

Samples were analysed using reads mapped to the GRCh38 (NCBI) human genome. Gene quantification was obtained after feature summarization with the RSubread package in R. Raw counts were normalized with *voom* and CPM values were log transformed to perform Principal Component Analysis (PCA). For each clustered group, expression levels from the dilated and the non-dilated zones were compared with controllevels. Using the *voom/limma* [11] pipeline in the R environment, DEGs were selected based on the following criteria: log fold change > 2, and adjusted p-value < 0.05 with Benjamini-Hochberg correction. Gene ontology analysis was performed using the GeneCodis tool [12]. Signalling pathway interaction analysis was performed with the SPIA package in R, using the fold change values from the obtained DEGs, with the following defaults: 4000 bootstrap iterations, Fisher's method to combine p-values, and NULL value for beta. MicroRNA Target prediction for the 3′UTR SNP identified in the two MFS patients was performed using a custom prediction with 50 nucleotides flanking the mutation region up- and downstream in the miRDB database for target prediction and functional annotations (www.mirdb.org/miRDB/).

3. Results

Four different *FBN1* mutations were identified in MFS samples of which one mutation was identical in patients M031d/nd and M054d/nd (Supplemental Table 1). This variant, located at the SNP site rs56194244 within the 3′UTR of *FBN1*, is reported with a prevalence of approximately 2% in the European population and has been associated with MFS (National Institute of Biotechnology Information, www.ncbi.nlm.nih.gov/variation/view/), however, there is no citation available. Furthermore, two MFS patients (M035 and M052) did not have any mutation detectable by RNA sequencing in the *FBN1* gene and more than one mutation in *FBN1* were seen in two patients (M054 and M057). These were two missense mutations with cysteine substitution,

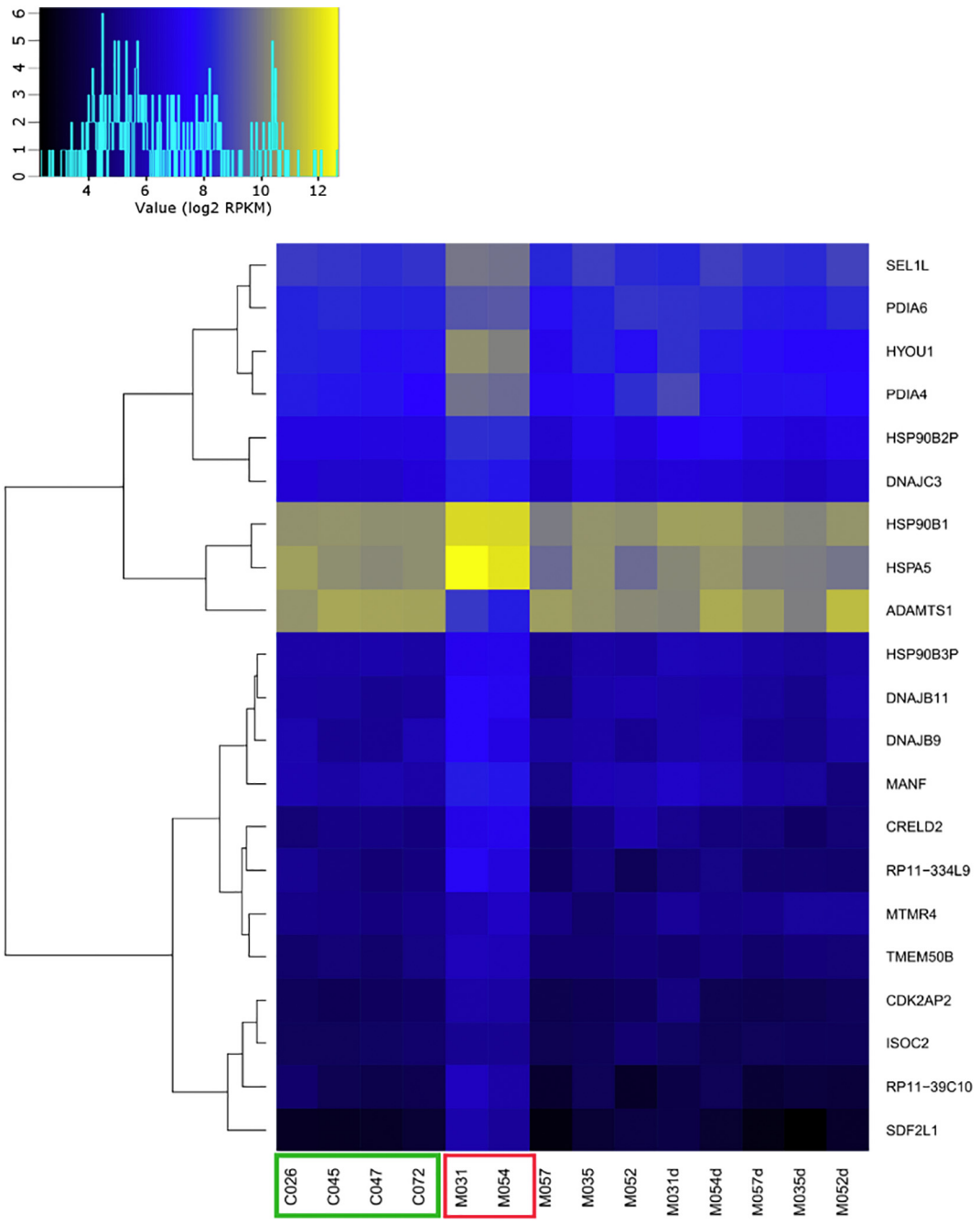

Fig. 1. Genes from the non-dilated aortic zone of 3′UTR FBN1 mutations are differentially expressed. Heat map of the 21 differentially expressed genes. MFSnd 3′UTR (red box, N = 2) expression levels were compared with control (green box, N = 4) expression levels. DEGs were selected based on the following criteria: adjusted p-value < 0.05 with Benjamini-Hochberg correction, and LFC > 2. Colour codes are representative for log2 RPKM (reads per kilobase-million). Counts range from low (black) to high (yellow).

one in addition to the 3′UTR *FBN1* mutation in patient M054 and the other in addition to an intronic mutation in patient M057 (Supplemental Table 1).

Due to the high variability within the MFS groups and the heterogeneity of mutations, patients were then grouped by mutation type. Six groups were established: MFS 3′UTR (M031and M054), MFS no mutation (M035 and M052) and MFS cysteine substitution (M054 and M057). The groups were further divided into dilated (d) and non-dilated (nd) zone samples. Neither the cysteine substitution nor the no mutation group showed significant changes in gene expression in either zone. However, 21 genes were differentially expressed in the nd zone of MFS patients with 3′UTR mutation (Fig. 1 and Table 1). Amongst the DEGs were transcripts for proteins involved in the ER stress response such as *SEL1L*, *MANF* and *CRELD2* as well as molecular chaperones *HSP90B1*, *HSPA5*, the DNAJ Heat Shock Proteins *DNAJB11*, *DNAJC3*, *DNAJB9* and Disulphide Isomerases *PDIA4* and *PDIA6*.

Enrichment analysis identified a specific cluster of Biological Processes (BP) associated with the catabolic cellular mechanisms involved with glycoprotein misfolding in the endoplasmic reticulum (ER). Amongst the most significant processes were *protein folding* (GO: 0006457), *ER-associated protein catabolic processes* (GO: 0030433) and *glycerol ether metabolic processes* (GO: 0006662) (Supplemental Fig. 1A). The elemental activities defined by Molecular Functions (MF) of the gene products were *misfolded protein binding* (GO: 0051787) and

Table 1
Differentially expressed genes in the non-dilated aortic zone of FBN1 3′UTR mutation.

Ensembl_ID	Chr	p. value	adj. p. val	Entrez_ID	Gene_Symbol	logFC
ENSG00000145050	3	1.51E−07	0.000881447	7873	MANF	2.218700236
ENSG00000203914	1	2.26E−07	0.000881447	343477	HSP90B3P	1.401730176
ENSG00000259706	15	2.66E−07	0.000881447	7190	HSP90B2P	1.512506073
ENSG00000184164	22	1.90E−06	0.00308846	79174	CRELD2	2.106644862
ENSG00000090520	3	2.04E−06	0.00308846	51726	DNAJB11	1.809949117
ENSG00000102580	13	2.17E−06	0.00308846	5611	DNAJC3	1.477015156
ENSG00000149428	11	2.07E−06	0.00308846	10525	HYOU1	2.271583263
ENSG00000215895	1	1.42E−05	0.014096289	400750	AL354702.7	2.101273797
ENSG00000128228	22	4.88E−06	0.00606918	23753	SDF2L1	2.452464154
ENSG00000142188	21	2.21E−05	0.018290602	757	TMEM50B	1.413483265
ENSG00000166598	12	9.41E−06	0.010390831	7184	HSP90B1	1.447354609
ENSG00000167797	11	3.81E−05	0.027051472	10263	CDK2AP2	1.472378972
ENSG00000108389	17	4.59E−05	0.03040555	9110	MTMR4	1.117620691
ENSG00000154734	21	1.94E−05	0.017550027	9510	ADAMTS1	−2.405840232
ENSG00000250746	4	6.38E−05	0.036255719	100288073	RP11-39C10.1	1.920543762
ENSG00000071537	14	5.47E−05	0.033970467	6400	SEL1L	1.313808596
ENSG00000044574	9	3.80E−05	0.027051472	3309	HSPA5	1.990675005
ENSG00000063241	19	8.97E−05	0.044360615	79763	ISOC2	1.046034128
ENSG00000128590	7	0.000103118	0.044578343	4189	DNAJB9	1.738096843
ENSG00000143870	2	9.37E−05	0.044360615	10130	PDIA6	1.044457326
ENSG00000155660	7	9.82E−05	0.044364931	9601	PDIA4	1.91095168

unfolded protein binding (GO: 0051082) as well as *heat shock protein binding* (GO: 0031072), *chaperone binding* (GO: 0051087), *protein disulphide isomerase* and *oxireductase* activity (GO: 003756 and GO: 0015035, respectively) (Supplemental Fig. 1B). Enrichment analysis identified the *ER* (GO: 005783), *ER-Golgi intermediate compartment* (ERGIC; GO: 005793) and the *melanosome* (GO: 0042470) as subcellular compartments (CC) of gene product activity (Supplemental Fig. 1C). In addition, the Kyoto Encyclopedia of Genes and Genomes (KEGG) pathway maps identified targets involved in *Protein processing in the Endoplasmic reticulum* as molecular network (Fig. 2A). The Signalling Pathway Impact Analysis (SPIA) [13] identified the most relevant altered cellular pathways due to 3′UTR *FBN1* mutation. Thus, *Protein processing at the Endoplasmic reticulum* (*ER*) *stress* (Fig. 2B) was significantly activated in the 3′UTR MFSnd samples (p-value = 1.10×10^{-7}). More specifically, our identified DEGs were involved in protein recognition by luminal chaperones and protein targeting of terminally misfolded and accumulated proteins leading to ER-associated protein degradation (ERAD).

To verify our RNAseq results, we analysed target genes involved in the ER stress downstream signalling by quantitative RT-PCR. Results showed an increased expression of *MANF*, *HSPA5*, *SEL1L*, *DDIT3/CHOP* and *CRELD2* in the non-dilated zone of MFS patients with 3′UTR mutation (Fig. 3). No statistical differences were observed for *ATF4*, *ATF6* and *ERN1*, but both *ATF4* and *ERN-1* showed a clear trend to increase (p = 0.0508 and p = 0.0513, respectively) (Fig. 3 and Supplemental Fig. 2A).

We next evaluated in VSMC from MFS patients with 3′UTR mutation and controls, the protein levels of the ER stress markers BiP/GRP78, HSP90, ATF6, CHOP and sXBP1 (Fig. 4A). Results showed that BiP, CHOP and sXBP1 were significantly increased in VSMC from the non-dilated zone of MFS patients with 3′UTR mutation (Fig. 4A), while HSP90 and ATF6 (total and active forms) remained unchanged (Fig. 4A and Supplemental Fig. 2B, respectively) in both the dilated and the non-dilated aortic zone. Interestingly, CHOP protein levels also increased in the dilated zone of aorta, which was not observed for mRNA. Furthermore, we were interested to know whether this ER-associated stress response led to a reduction in protein translation through the activation of eIF2α. We analysed the ratio of phosphorylated (p) to non-phosphorylated eIF2α and we observed a significant decrease in Marfan VSMC with 3′UTR mutation in both the dilated and non-dilated aneurysmal zone (Fig. 4B).

As 3′UTRs are major binding sites for micro RNAs (miRNAs) that repress the target mRNA, we performed miRNA-binding prediction analysis of the *FBN1* 3′UTR. We found *miR-1252-5p* (NCBI gene ID: 100302136) to bind to the exact SNP site where *FBN1* 3′UTR was mutated at chr15:48409001 with a prediction score of 56 of 100. The highest scoring *FBN1*-binding miRNAs belonged to the family of *miR-29* (*miR-29a*, *miR-29b* and *miR29c*) which has previously been described to drive aneurysm formation in MFS [14].

4. Discussion

Due to the low prediction of disease outcome in MFS, many attempts have been made to correlate mutation types with disease progression. It was recently argued that detection of non-exonic mutation variants is limited by conventional molecular testing, which omits untranslated regions [9]. In addition, the current classification of HI and DN phenotype-causing mutations potentially reflects an incomplete image of disease causing variables. Here, we analysed 5 male MFS patients who represented a homogenous group with respect to organ involvement but showed heterogeneity of *FBN1* mutation types including their absence. In fact, even with a technique as powerful as RNA sequencing, we cannot exclude the possibility of deep intronic mutations in our samples. Strikingly, given the low recurrence of identical *FBN1* mutations, in two patients we found a mutation in the *FBN1* 3′UTR, which has not been previously reported in MFS. Even though this mutation has been annotated as being more frequent in the general population, Marfan patients with this mutation showed a clear molecular profile and the mutation was absent in the control group. Furthermore, mutations in 3′UTRs have been demonstrated to be critical gene locations in congenital heart diseases [16].

Pathway analysis predicted a strong activation of the UPR in VSMC from the non-dilated aortic zone in patients with 3′UTR mutation, including the increased expression of cell stress-associated chaperones, ERAD, and facilitators of protein degradation in a ubiquitin-dependent manner. Transcriptional expression and protein analysis confirmed the occurrence of ER stress in association with 3′UTR mutation. Increased protein levels of BiP/GRP78, CHOP and sXBP1 verify the previous results, indicating the activation of UPR signalling pathways through the IRE1-XBP1 pathway in the non-dilated zone of *FBN1* 3′UTR mutation MFS patients. Intriguingly, the ER stress profile was mostly present in the non-dilated aortic zone, suggesting a transient stress response as seen previously in a model of cardiac fibrosis, indicating a persistent remodelling of the affected tissue from a very early disease stage on

A

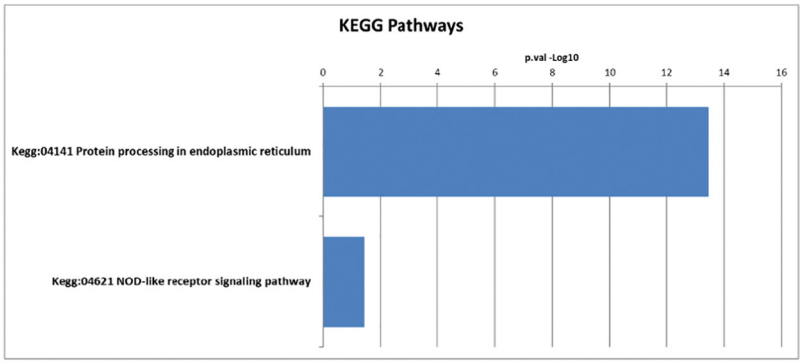

B

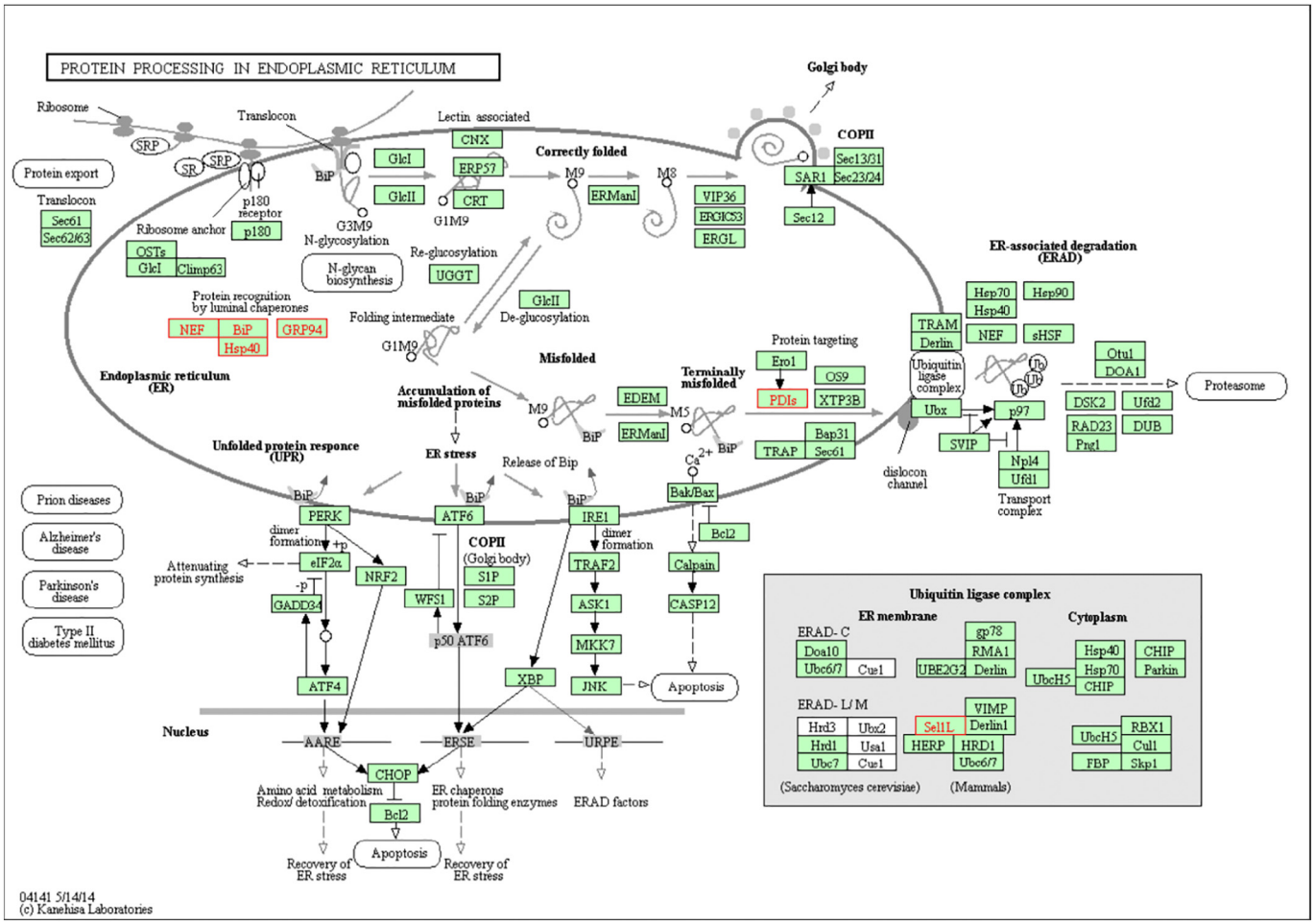

Fig. 2. KEGG pathway Map and SPIA analysis of most relevant altered pathways in VSMC from the non-dilated zone of 3′UTR FBN1 mutation. (A) KEGG pathway enrichment analysis identifies protein processing in the endoplasmic reticulum as the molecular network involving the DEG of the 3′UTR *FBN1* mutation in the non-dilated aortic zone (N = 2). (B) SPIA visual map of the intracellular molecular network affected by the 3′UTR *FBN1* mutation in the non-dilated aortic zone (N = 2).

[17]. However, at the protein level, the increased UPR signalling through CHOP persisted well into the diseased tissue stage of the dilated aorta, indicating that even though the tissue remodelling takes place in early stages, the effector protein activation persists.

The decreased phosphorylation of eIF2α indicates that the general protein translation machinery is in fact augmented despite the increased response to unfolded or accumulated protein. It is possible that abnormally folded fibrilin-1 protein accumulates in the ER without showing sequence mutations, which potentially circumvents the global reduction of translation through eIF2α phosphorylation, leading to the demonstrated UPR/ER stress profile. Interestingly, ER stress, as opposed to the mutant protein itself, has recently been suggested to be an alternative mediator of disease outcome by inducing cardiac remodelling and fibrosis through cellular apoptosis and alterations in signalling pathways [18]. In addition, the specific 3′UTR mutation described here is predicted to lead to a loss of a binding site for miRNA, which in turn

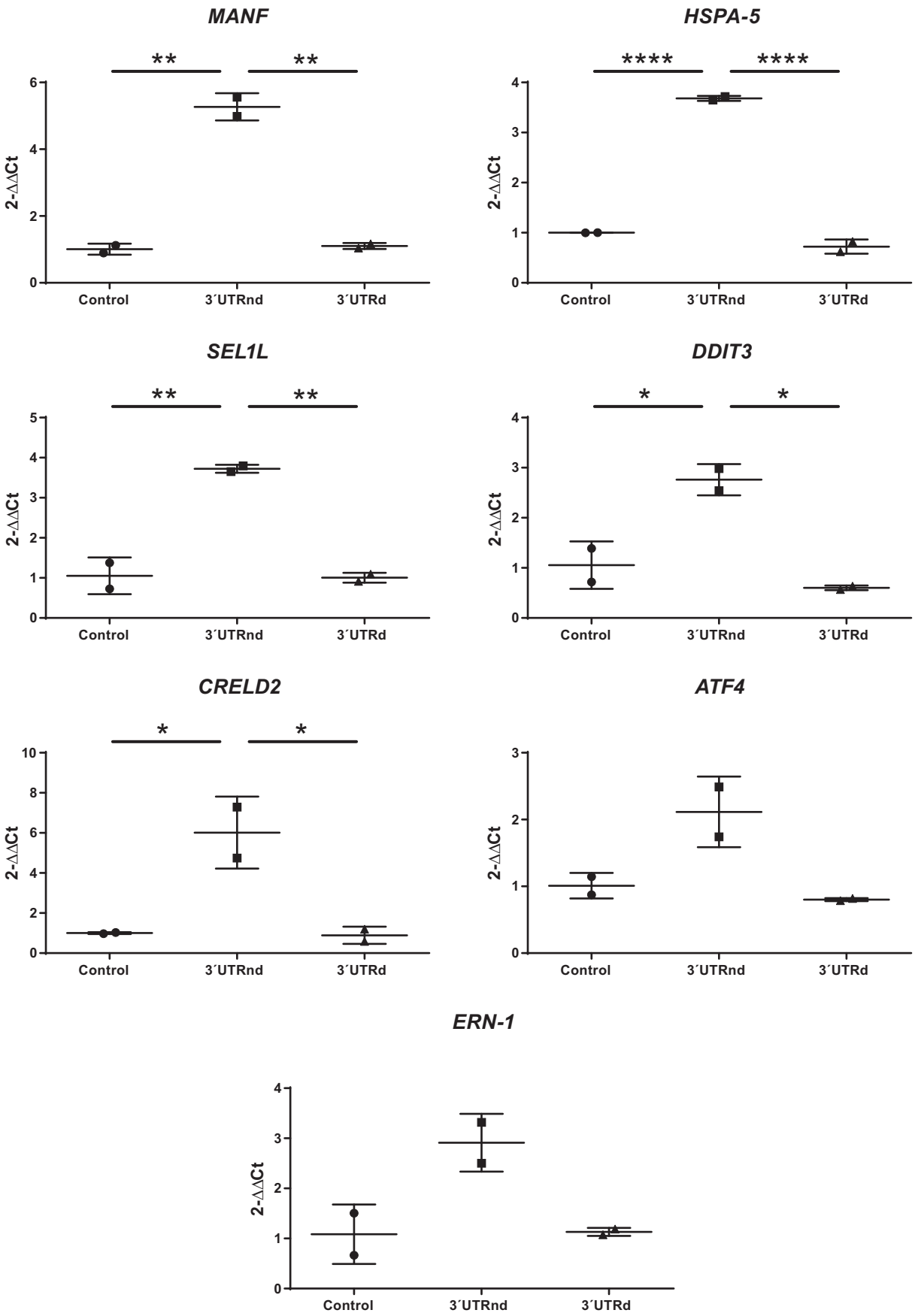

Fig. 3. ER stress mediators at the transcriptional level in VSMC from Marfan patients with a 3′UTR *FBN1* mutation. (A) Quantitative RT-PCR analysis of key factors MANF, HSPA5, SEL1L, DDIT3, CRELD2, ATF4 and ERN1 in the ER stress response to unfolded protein shows an upregulation in non-dilated zone of aortic VSMC in patients with 3′UTR *FBN1* mutation (N = 2). Statistical analysis was performed by ANOVA with Tukey's multiple comparison post hoc test. Shown are means with standard deviation. *p ≤ 0.05; **p ≤ 0.005; ****p ≤ 0.0001.

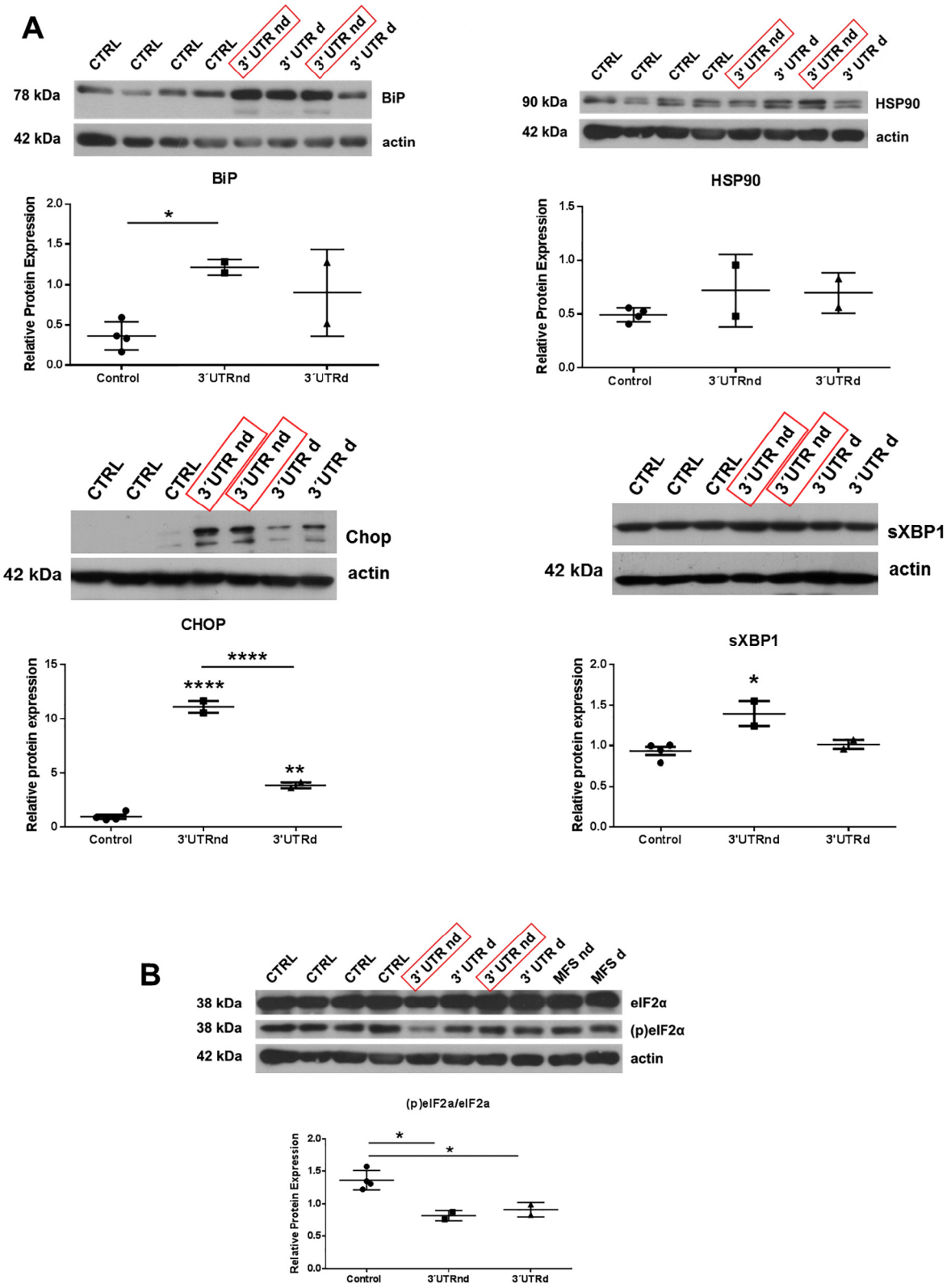

Fig. 4. ER stress mediators protein levels and protein translation machinery in VSMC from Marfan patients with a 3′UTR *FBN1* mutation. (A) Upregulation of key proteins involved in the UPR such as BiP/GRP78, CHOP and sXBP1 in the non-dilated zone of 3′UTR *FBN1* mutated VSMC as indicated by red boxes (Control N = 3–4; FBN1 3′UTR N = 2). Statistical analysis was performed by ANOVA with Tukey's multiple comparison post hoc test. Shown are means with standard deviation. *p ≤ 0.05; **p ≤ 0.001; ****p ≤ 0.0001. (B) Decreased ratio of phosphorylated (p)eIF2α in the dilated and non-dilated zone in FBN1 3′UTR mutated VSMC (Control N = 4; FBN1 3′UTR N = 2, $p < 0.05$). Statistical analysis was performed by ANOVA with Tukey's multiple comparison post hoc test. Shown are means with standard deviation. *p ≤ 0.05.

might then lead to a loss of post-transcriptional regulation and FBN1 protein accumulation in the ER. MicroRNA deregulation is a scarcely studied but intriguing new field in MFS due to the recently discovered *miR-29*, which specifically targets ECM genes [14]. *miR1252-5p* and its variant SNP sites in *FBN1* could be a gene prediction marker of aortic risk in MFS, similar to a recent large scale study of SNP variants in ovarian cancer. In this particular case, variants of *miR-1252-5p* binding sites in ovarian cancer-associated genes have been shown to be predictive markers of cancer progression due to the critical role of the 3′UTR in oncogenesis [15]. Further research of miRNA involvement and their deregulation through 3′UTR mutations could be an interesting tool to elucidate the disease development of MFS.

5. Conclusions

We here identified a 3′UTR mutation of *FBN1* in MFS patients with aortic rupture, which converges on processes that produce ER stress. Our results strongly suggest that *FBN1* 3′UTR mutations are involved in aortic aneurysm formation in MFS patients. The inclusion of non-coding *FBN1* 3′UTR regions as a diagnostic criterion could provide new insights into novel patient clusters and genetically unresolved cases, potentially improving the thus far incomplete view of genotype-phenotype correlation.

Transparency document

The Transparency document associated with this article can be found, in online version.

Acknowledgements

The authors would like to thank Marta Gut from the CNAG for her assistance in methodological questions as well as Maite Muñoz and Laura Barberà for technical assistance. This work was supported by grants to G.E. (SAF 2015-64136-R and SAF 2017-80309-R). M.G. is supported by the Miguel Servet Program (ISCIII; CP15/00126). The support of the NMF to GE is acknowledge.

Appendix A. Supplementary data

Supplementary data to this article can be found online at https://doi.org/10.1016/j.bbadis.2018.10.029.

References

[1] H.C. Dietz, et al., Marfan syndrome caused by a recurrent de novo missense mutation in the fibrillin gene, Nature 352 (1991) 337–339.
[2] E.R. Neptune, et al., Dysregulation of TGF-beta activation contributes to pathogenesis in Marfan syndrome, Nat. Genet. 33 (2003) 407–411.
[3] D.M. Milewicz, Treatment of aortic disease in patients with Marfan syndrome, Circulation 111 (2005) e150–e157.
[4] G. Collod-Beroud, et al., Update of the UMD-FBN1 mutation database and creation of an FBN1 polymorphism database, Hum. Mutat. 22 (2003) 199–208.
[5] R. Franken, et al., Relationship between fibrillin-1 genotype and severity of cardiovascular involvement in Marfan syndrome, Heart (22) (2017) 1795–1799.
[6] B.J. Landis, G.R. Veldtman, S.M. Ware, Genotype – phenotype correlations in Marfan syndrome, Heart 22 (2017) 1750–1752.
[7] R. Franken, et al., Genotype impacts survival in Marfan syndrome, Eur. Heart J. (43) (2016) 3285–3290.
[8] K.A. Groth, et al., Evaluating the quality of Marfan genotype-phenotype correlations in existing FBN1 databases, Genet. Med. 19 (2017) 772–777.
[9] E. Gillis, et al., An FBN1 deep intronic mutation in a familial case of Marfan syndrome: an explanation for genetically unsolved cases? Hum. Mutat. 35 (2014) 571–574.
[10] E. Crosas-Molist, et al., Vascular smooth muscle cell phenotypic changes in patients with Marfan syndrome, Arterioscler. Thromb. Vasc. Biol. (4) (2015) 960–972.
[11] M.E. Ritchie, et al., limma powers differential expression analyses for RNA-sequencing and microarray studies, Nucleic Acids Res. 43 (2015) e47.
[12] D. Tabas-Madrid, R. Nogales-Cadenas, A. Pascual-Montano, GeneCodis3: a non-redundant and modular enrichment analysis tool for functional genomics, Nucleic Acids Res. 40 (2012) W478–W483.
[13] A.L. Tarca, et al., A novel signaling pathway impact analysis, Bioinformatics 25 (2009) 75–82.
[14] D.R. Merk, et al., miR-29b participates in early aneurysm development in Marfan syndrome, Circ. Res. (2) (2012) 312–324.
[15] X. Chen, et al., Targeted Resequencing of the MicroRNAome and 3′UTRome Reveals Functional Germline DNA Variants With Altered Prevalence in Epithelial Ovarian Cancer, 34 (2014), pp. 2125–2137.
[16] S.M. Reamon-Buettner, S.-H. Cho, J. Borlak, Mutations in the 3′-untranslated region of GATA4 as molecular hotspots for congenital heart disease (CHD), BMC Med. Genet. 8 (38) (2007).
[17] J. Groenendyk, et al., Inhibition of the unfolded protein response mechanism prevents cardiac fibrosis, PLoS One 11 (2016) 1–15.
[18] R.P. Boot-Handford, M.D. Briggs, The unfolded protein response and its relevance to connective tissue diseases, Cell Tissue Res. 339 (2010) 197–211.